Gas Permeation and Selectivity of Poly(organophosphazene) Membranes†

Harry R. Allcock,* Constance J. Nelson, William D. Coggio, and Ian Manners

Department of Chemistry, The Pennsylvania State University, University Park, Pennsylvania 16802

William J. Koros,* David R. B. Walker, and Luiz A. Pessan

Department of Chemical Engineering, The University of Texas at Austin, Austin, Texas 78712-1062

Received August 25, 1992; Revised Manuscript Received November 12, 1992

ABSTRACT: A series of poly(organophosphazenes) with the general structure $[NP(R)_x(OC_6H_5)_{2-x}]_n$, where $x \leq 2$ and R = $OC_6H_4SiMe_3$, $OC_6H_4SiMe_2Ph$, $OC_6H_4SiMePh_2$, OC_6H_4Br, and OCH_2CF_3, and the ferrocenyl polymer $[N_3P_3(OCH_2CF_3)_4(\eta\text{-}C_5H_4)_2Fe]_n$ were synthesized. Molecular structural characterization for these polymers was achieved by ^1H and ^{31}P NMR, gel permeation chromatography, elemental microanalysis, and differential scanning calorimetry. Films of these polymers were examined with respect to their permeability to O_2, N_2, CO_2, He, and CH_4, and selectivity ratios were established. The effect of cross-linking on both the permeation and selectivity values for films of the silyl-bearing polymers was also investigated. The change in permeability and selectivity as a function of side group structure variations, free volume effects, gas pressure, and glass transition temperature (T_g) is discussed. Poly[bis(trifluoroethoxy)phosphazene] was found to have oxygen permeabilities comparable to those of poly(dimethylsiloxane) but with higher permselectivities.

The development of novel membrane materials is a subject on which much future technology depends. Such materials have possible uses in biotechnology, pharmaceutical synthesis, biomedicine, bioreactors, and gas separation sciences.[1] One of the most significant challenges inherent in the design of new membranes is the need to combine high intrinsic permeability with high selectivity. Moreover, significant progress in membrane separation technology depends not only on the preparation of new materials but also on elucidation of the mechanisms for gas transport. Progress is impeded at present by an insufficient understanding of the relationships between the chemical structure of a polymer and its gas transport properties.[2,3]

As noted by Stern,[3] few studies on the structure–permeability relationships of rubbery polymers have been published. Thus in this study we planned to establish a basis set of data on these relationships for phosphazene polymers. Specifically, the gas permeability of several poly(organophosphazenes) (1) was investigated as a function of side group structure. Polyphosphazenes are especially suited for such a study because the properties of the polymers can be fine-tuned by changes in side group structure, a process that is facilitated by the macromolecular substitution route used for their preparation.[4] Thus, in theory, these polymers might be tailored to optimize both gas permeability and selectivity.

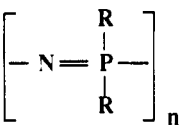

1

To date there have been comparatively few investigations of the gas permeabilities of phosphazene polymers.[5] Hirose and co-workers have studied poly[bis(trifluoroethoxy)phosphazene] (5) extensively both above and below its mesomorphic transition temperature T(1).[5d,e] However, the history and morphology of the polymer films studied in those investigations differed markedly from those of the polymer membranes prepared for this study. Thus the results from those studies are not directly comparable with those reported here.

In this work, a representative series of poly(organophosphazenes) was synthesized (see Chart I) and their gas permeability and selectivity values were determined. The fluoroalkoxy single-substituent polymer **5** was selected as a control material. Polymers with phenoxy side groups were used because of the known ability of these groups to enhance film formation. A mixed-substituent aryloxy–fluoroalkoxy polymer **4** was examined because of its low degree of microcrystallinity. The polymer bearing ferrocenyl groups (**14**) has been shown previously to possess redox conductive properties[6] and was used to examine the possibility of facilitated transport.[7] Thus, an attempt was made to probe the role played by the metal-containing side group and the possibility that a connection may exist between oxidation state and selectivity for a polymer of this type.

For the silyl-bearing polymers **8–10**, the choice of organosilicon side groups (R) was based on the idea that organosilicon units may favor high gas permeability. It is known that organosiloxane polymers are highly gas permeable, particularly toward oxygen, and thermally and oxidatively stable.[8] Thus, in this work we investigated the possibility that the linkage of organosilicon groups to polyphosphazenes might enhance both the oxygen permeability and selectivity of the resultant polymer membranes.

The movement of gases through polymer membranes was first explained by Graham in 1866.[9] This phenomenon was described as the condensation and dissolution of a gas at one surface followed by diffusion through the material as a liquid and evaporation to the gaseous state at the opposite surface. Several fundamental factors influence gas transport through a polymeric membrane. The

* Authors to whom correspondence should be addressed.

† This work was presented in a talk given at the 204th National Meeting of the American Chemical Society in Washington, DC, August 1992.

0024-9297/93/2226-1493$04.00/0

Chart I

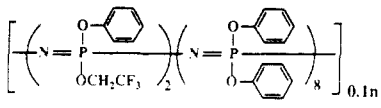

4

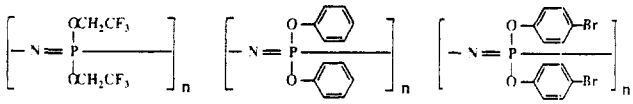

5 6 7

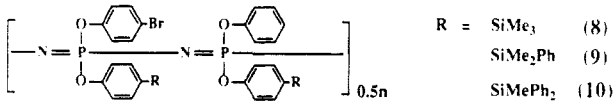

R = $SiMe_3$ (8)
$SiMe_2Ph$ (9)
$SiMePh_2$ (10)

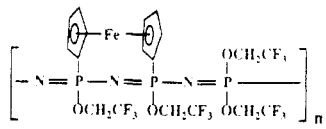

14

concentration and nature (size, shape, polarity) of the permeant molecule in the polymer membrane are important. In addition, the temperature at which the system is examined plays a key role. Finally, the nature of the polymer itself, its chain flexibility, polarity, crystallinity, and molecular structure are determining factors.[10]

Historically, dimethylsiloxane polymers have shown the highest oxygen permeability coefficients.[11] For example, poly(dimethylsiloxane) has a P_{O_2} value in the range of 600 barrers (unit barrers = 10^{-10} $cm^3 \cdot cm/cm^2 \cdot s \cdot cmHg$). However, this polymer has a low oxygen selectivity, with a P_{O_2}/P_{N_2} ratio of approximately 2.[12] The high gas permeabilities of organosiloxane polymers can be attributed in part to the flexibility of the polymer backbone and the resultant high free volume. However, rubber elasticity is an experimental impediment to asymmetric membrane fabrication. One proposed solution to this problem involves the use of polymers that have relatively rigid chain structures but flexible side groups. By this means, in theory, a processable, highly gas permeable polymer might be accessible. However, the synthesis of such polymers is, in general, quite difficult.[12] Recently, Masuda and Higashimura et al. reported the synthesis of tractable silicon-containing poly(diphenylacetylenes) with remarkable oxygen permeabilities.[13]

The polyphosphazene backbone resembles the polysiloxane backbone in chain flexibility.[4] A disadvantage of polysiloxanes is the limited range of organic side groups that can be incorporated into the molecular structure. Modification of poly(organosiloxanes) by macromolecular reactions is hindered by the sensitivity of the backbone bonds to cleavage reactions.[14] However, the properties of polyphosphazenes can readily be tailored by a choice of side group structure. Thus the processability and subsequent fabrication of polyphosphazenes can be controlled by changes in the macromolecular substitution reactions on which their synthesis depends. Additional modification of the organic side groups can also be carried out to optimize the final permeation and selectivity of the polymers and to gain an insight into the role played by these substituents. This approach is illustrated with respect to the organosilicon derivatives 8–10.

Results and Discussion

General Overview. The poly(organophosphazene) membranes investigated in this work gave a range of gas permeability and selectivity values that depended on side group structure (see Tables II and III). First, several general features were varied for the polymer structures to test the applicability of current hypotheses. Polymers with bulky side units are expected to show high oxygen permeability values.[12] However, this trend was not found for polyphosphazenes. In fact, the fluoroalkoxy phosphazene polymer, 5, showed a 50-fold increased permeability to oxygen compared to the phenoxy polymer, 6. For the silyl-bearing polymer series (8–10) a clear trend was observed. As the incorporation of bulky phenyl groups attached to silicon increased, the permeability of the membranes to all of the gases decreased. This decrease in gas permeability was accompanied by a corresponding increase in selectivity.

A possible explanation is the known tendency of phenyl groups to align or stack within a solid material to favor an aggregated membrane structure, a condition unfavorable for gas permeation.[12] The permeation data obtained for polymer 7 provide an example. This polymer might be expected to undergo aggregation because of the presence of the aryloxy groups. Furthermore, this tendency could be enhanced by the polarity induced by the para-substituted halogen group.[15] Indeed, the measured permeation values for polymer 7 were the lowest found in this study.

Second, previous results predict an increase in gas permeation with decreasing polymer density, which may be a function of the packing of the phosphazene polymer chains.[5c] Such a trend was detected in this study for the organosilyl-bearing polymers (see Table III). An increase in density and corresponding decrease in gas permeation with higher incorporations of phenyl side groups was found. However, consideration of the concurrent increase in fractional free volume would make the decrease in permeability an unexpected result.

Third, polymer molecular weight affects gas permeation and selectivity. Studies carried out with substituted polyacetylenes have shown that both oxygen permeability and selectivity increase and gradually level off with increasing polymer molecular weight. Therefore it is desirable to use polymers with the highest possible molecular weights for efficient gas enrichment and separation.[16] The materials discussed here are all high polymers with M_w values in the range of 10^6.

Overall, the values obtained indicate very high diffusion coefficients for the phosphazene polymers. In the following sections the relationship of the measured gas permeabilities and calculated selectivities to the polymer structure will be discussed. In addition, the role of free volume will be considered, particularly with regard to cross-linked membranes.

Polymer Synthesis and Characterization. The syntheses of the mixed-substituent trifluoroethoxy–phenoxy phosphazene polymer (4), poly[bis(trifluoroethoxy)phosphazene] (5), poly[diphenoxyphosphazene] (6), and poly[bis(*p*-bromophenoxy)phosphazene] (7) were carried out as described in the Experimental Section in a manner similar to previously published methods (see Scheme I).[17,18]

Poly(lithiophenoxyphosphazene) was prepared by the known metal–halogen exchange reaction of poly[bis(*p*-

Scheme I

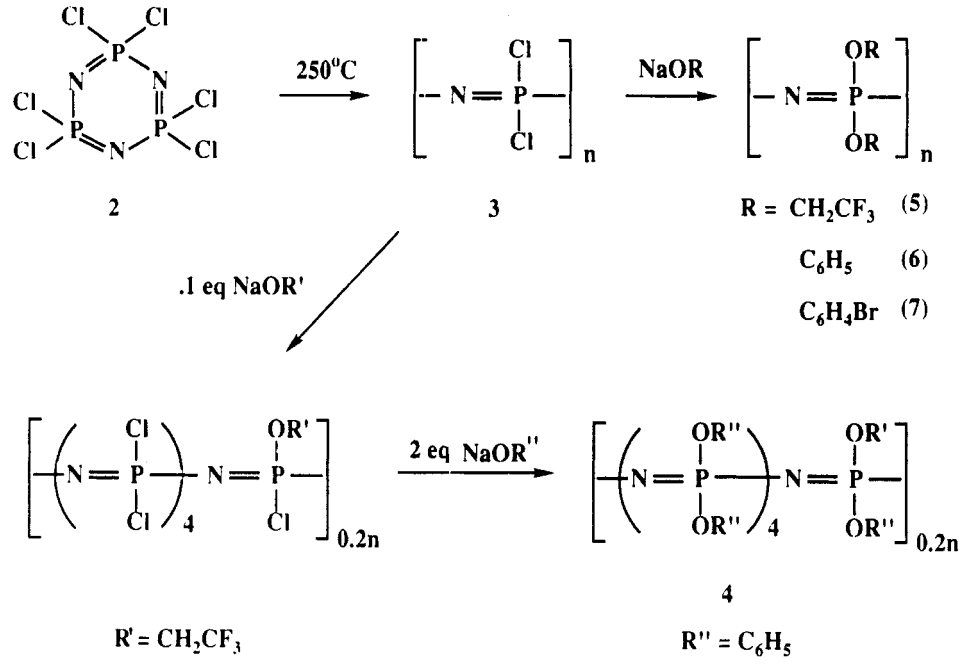

Scheme II

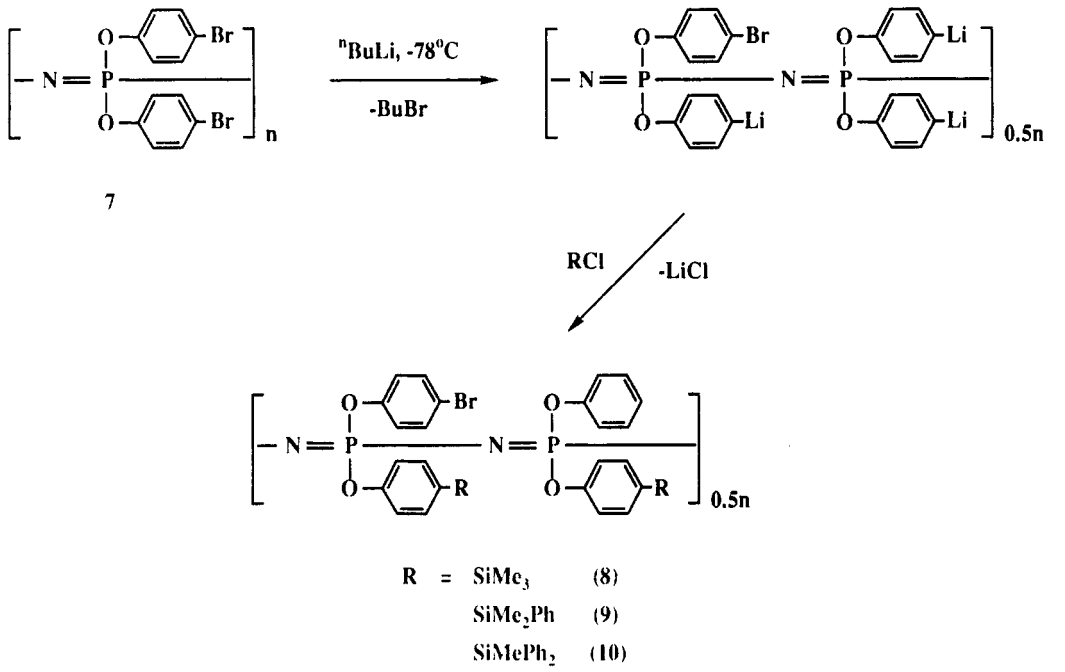

bromophenoxy)phosphazene] (7) with *n*-BuLi at −78 °C (see Scheme II).[18,19] The lithioaryloxy intermediate is extremely sensitive to trace amounts of water, and extreme care must be taken to protect this intermediate from moisture. In addition, at high levels of lithiation, the polymer becomes insoluble in THF, presumably a consequence of the increased ionic character of the macromolecules. Thus, the efficiency of the lithiation process may be impaired, and this may influence the effectiveness of the metal–halogen exchange reaction.

The lithiated polymer was then subsequently allowed to react with $ClSiMe_3$, $ClSiMe_2Ph$, and $ClSiMePh_2$ to yield the corresponding poly(organosilylphosphazenes) (8–10).[20] As shown in Table I, the incorporation of the organosilyl units decreased with increases in the number of phenyl groups in the chlorosilane, presumably for steric reasons. Thus the side groups of the final polymers 8–10 bore 90%, 60%, and 45% organosilicon-aryloxy units, with the remainder being unreacted bromophenoxy and phenoxy units, formed by deactivation of the aryllithium units by traces of water.

The transannular ferrocenyl polyphosphazene (14) was synthesized via the ring-opening polymerization of the substituted trimer 13 by methods described by Allcock, Dodge, Manners, and Riding (see Scheme III).[21] Polymerization of a trimer that contained no phosphorus–halogen bonds was possible because of the ring strain imparted by the bridging ferrocenyl group.

The polymer structures were examined with the use of ^{31}P (36.2 MHz) and ^{1}H (360 MHz) NMR spectroscopy, elemental microanalysis, gel permeation chromatography, and differential scanning calorimetry (see Table I and the Experimental Section). ^{1}H NMR spectroscopy and elemental microanalysis were used in tandem to estimate the ratios of the different side groups in the mixed-substituent polymers. For the organosilyl polymers, the ^{1}H NMR spectra were utilized to establish the ratio of

Table I
Characterization Data for $[NP(R)_x(OC_6H_5)_y(OC_6H_4Br)_z]_n$

compd	R	x	y	z	signal	^{1}H NMR (δ, $CDCl_3$)	$10^{-5}M_n$	$10^{-6}M_w$	T_g (°C)
4	OCH_2CF_3	0.40	1.53	0	phenoxy	7.1–6.7 (9 H)	0.4	1.9	−10
					OCH_2CF_3	3.8–3.6 (1 H)			
5	OCH_2CF_3	2.00	0	0	OCH_2CF_3	4.4–4.2	3.7	2.0	−65
6	Cl	0.06	1.94	0	phenoxy	7.2–6.8	0.4	1.7	−6
7	Cl	0.01	0	1.99	phenoxy	7.1–6.9 (2 H)	12.0	2.5	10[a]
						6.6–6.4 (2 H)			
8	$OC_6H_4SiMe_3$	1.80	0.10	0.07	phenoxy	7.1–6.6 (8 H)	9.4	2.1	24[a]
					SiMe	+0.2 to −0.1 (17 H)			
9	$OC_6H_4SiMe_2Ph$	1.20	0.32	0.45	phenoxy	7.4–6.8 (6 H)	5.1	1.0	10[a]
					SiPh	6.8–6.3 (6 H)			
					SiMe	0.4–0.1 (7 H)			
10	$OC_6H_4SiMePh_2$	0.90	0.57	0.50	phenoxy	7.4–6.8 (9 H)	7.8	1.7	43[a]
					SiPh	6.8–6.3 (12 H)			
					SiMe	0.7–0.4 (4 H)			
14	$(OCH_2CF_3)_4(\eta\text{-}C_5H_4)_2Fe$				η-H's and OCH_2CF_3	5.0–4.1 (16 H)	1.4	2.0	61

[a] DSC analysis of polymers 7–10 also showed T_1 type transitions: for 7 (146 °C), for 8 (158 °C), for 9 (not observed), and for 10 (58 °C).

Scheme III

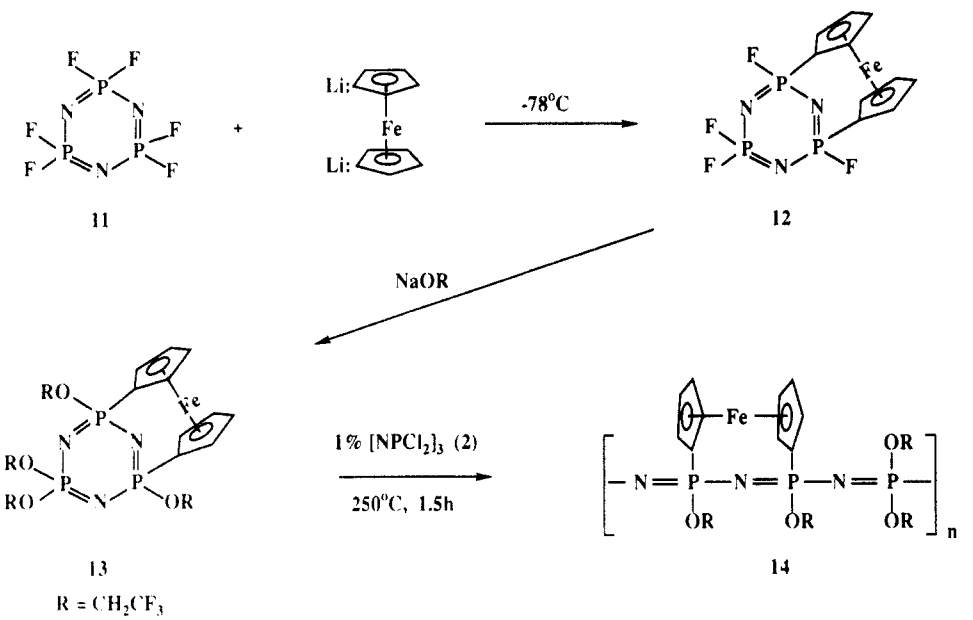

methyl to phenyl protons, and these data formed the basis of the calculated elemental microanalysis values.

Polymer Thermal Behavior. The glass transition temperatures (T_g) of the poly(organophosphazenes) used in this work were determined by differential scanning calorimetry (see Tables I and III). The linkage of organosilicon units to the aryloxy phosphazene induced a change in the physical properties of the polymers 8–10. The precursor polymer 7 is a microcrystalline material with a T_g of 10 °C and a T_1 transition at 146 °C. Incorporation of the $SiMe_3$, $SiMe_2Ph$, and $SiMePh_2$ units imparted a stiff elastomeric character to the polymers. The T_g of polymer 8 increased to 24 °C with a 90% organosilyl unit incorporation, and polymer 10 bearing only 45% silyl groups showed an increase to 43 °C.

Polymers 7–10 were found to be thermally stable when heated to temperatures near 350 °C and, with the exception of polymer 9, showed evidence of T_1 type transitions. Films of the silyl-bearing polymers (8–10) underwent cross-linking when exposed to 3 Mrads of ^{60}Co γ-irradiation, probably via a free radical cleavage of the aliphatic carbon–hydrogen bonds.[22,23] The thermal behavior of these cross-linked films (designated as 8*–10*) was also investigated; however, no significant change in the measured T_g's was detected. This is characteristic of lightly cross-linked materials. Polymers 8–10 and 8*–10* were also examined via hot stage microscopy; all the polymer films showed some optical birefringence under cross-polarized light.

Gas Permeability Studies: Theory. Previous studies indicate that a tradeoff exists between permeability and selectivity; that is, materials with high permeabilities usually possess low selectivities and vice versa. However, the main need in membrane-based gas separations is for novel polymeric materials that have both high permeability and good selectivity.

Permeability can be separated into diffusion and solubility coefficients as shown in eq 1.[24,25] The diffusion

$$P = DS \tag{1}$$

coefficient is kinetic in nature and is related to the size and shape of the guest small molecule and the molecular mobility of the polymer molecules. The solubility coefficient is thermodynamic in nature and is related to polymer–penetrant interactions and the condensability of the penetrant. The solubility coefficient is determined as the secant slope of the sorption isotherm when the downstream pressure is negligible compared to the upstream pressure,

$$S = C/p \tag{2}$$

where S is the solubility coefficient and C is the sorption level at the upstream feed pressure, p, of the penetrant.

Penetrants with higher critical temperatures tend to be more soluble in the absence of specific polymer–penetrant

Table II
Gas Permeation and Selectivity Data[a]

		permeability					selectivity			
polymer	press. (atm)	CO_2	O_2	He	N_2	CH_4	O_2/N_2	He/CH_4	CO_2/CH_4	N_2/CH_4
4	2	72.6	10.4	21.1	3.4	9.0	3.1	2.4	8.1	0.38
	5	76.4	10.5	21.1	3.5	8.9	3.1	2.4	8.6	0.39
	10	79.5	10.6	20.8	3.4	8.9	3.1	2.3	9.0	0.38
5	2	577.7	116.0	267.9	51.9	57.7	2.2	4.6	10.0	0.90
	5	595.2	117.7	265.5	53.8	62.3	2.2	4.3	9.6	0.86
	10	662.3	118.0	262.4	51.2	62.8	2.3	4.2	10.6	0.82
6	2	17.2	2.2	10.3	0.60	1.4	3.7	7.4	12.3	0.43
	5	—	2.1	9.6	0.50	1.3	4.2	7.4	—	0.38
	10	12.3	—	8.7	0.50	1.2	—	7.3	10.3	0.42
7	2	4.1	0.91	5.8	0.18	0.35	5.0	16.4	11.7	0.52
	5	4.6	0.88	5.8	0.18	0.36	4.9	16.1	12.7	0.49
	10	5.2	0.84	5.8	0.17	0.37	4.9	15.6	14.2	0.46
8	2	116.1	30.7	—	9.4	23.3	3.3	—	5.0	0.40
	5	124.4	30.2	61.8	9.0	23.3	3.4	2.6	5.3	0.39
	10	139.8	29.7	60.4	8.6	24.0	3.5	2.5	5.8	0.36
9*	2	44.8	7.8	20.7	2.2	5.8	3.6	3.6	7.8	0.37
	5	48.8	7.9	20.6	2.2	5.8	3.6	3.6	8.4	0.38
	10	53.3	7.7	20.1	2.1	5.8	3.6	3.5	9.3	0.37
10	2	5.6	1.3	10.5	0.31	0.43	4.2	24.3	13.1	0.72
	5	6.1	1.3	10.6	0.27	0.39	4.6	27.1	15.5	0.70
	10	7.2	1.3	10.4	0.25	0.38	5.1	27.2	18.7	0.65
14	2	60.6	15.0	83.1	4.7	5.1	3.3	16.3	11.9	0.91
	5	67.0	15.4	83.0	4.5	5.1	3.4	16.2	13.0	0.87
	10	91.2	15.1	82.3	4.4	5.1	3.4	15.9	17.6	0.85

[a] Permeability is in barrers = 10^{-10} $cm^3 \cdot cm/cm^2 \cdot s \cdot cmHg$; all measurements were made at a constant temperature of 35 °C; (—) indicates nonreproducible measurements; * indicates values for cross-linked films.

Table III
Gas Permeation and Selectivity Data for the Organosilyl-Bearing Polymers[a]

		polymer				
	atm	8	8*	9*	10*	10
density		1.1135	1.1140	1.2331	1.2600	1.2323
frac free vol		0.1696	0.1693	0.1827	0.1926	0.2104
			Permeability			
CO_2	2	116.1	116.3	44.8	2.8	5.6
	5	124.4	125.6	48.8	3.1	6.1
	10	139.8	141.2	53.3	3.7	7.2
O_2	2	30.7	31.3	7.8	0.69	1.3
	5	30.2	30.8	7.9	0.67	1.3
	10	29.7	29.7	7.7	0.69	1.3
He	2	—	60.3	20.7	6.4	10.5
	5	61.8	60.2	20.6	6.4	10.6
	10	60.4	59.9	20.1	6.4	10.4
N_2	2	9.4	8.8	2.2	0.11	0.31
	5	9.0	8.7	2.2	0.12	0.27
	10	8.6	8.6	2.1	0.12	0.25
CH_4	2	23.3	22.7	5.8	0.17	0.43
	5	23.3	23.3	5.8	0.18	0.39
	10	24.0	23.7	5.8	0.19	0.38
			Selectivity			
O_2/N_2	2	3.3	3.6	3.6	6.0	4.2
	5	3.4	3.5	3.6	5.7	4.6
	10	3.5	3.4	3.6	5.9	5.1
He/CH_4	2	—	2.7	3.6	36.9	24.3
	5	2.6	2.6	3.6	35.6	27.1
	10	2.5	2.4	3.5	34.2	27.2
CO_2/CH_4	2	5.0	5.1	7.8	15.9	13.1
	5	5.3	5.4	8.4	17.5	15.5
	10	5.8	6.0	9.3	19.9	18.7
N_2/CH_4	2	0.40	0.39	0.37	0.66	0.72
	5	0.39	0.37	0.38	0.66	0.70
	10	0.36	0.36	0.37	0.63	0.65

[a] Permeability is in barrers = 10^{-10} $cm^3 \cdot cm/cm^2 \cdot s \cdot cmHg$; all measurements were made at a constant temperature of 35 °C; (—) indicates nonreproducible measurements; * indicates values for cross-linked polymer films. Measured T_g values for the cross-linked polymers were 8* = 25 °C; 9* = 11 °C, and 10* = 43 °C.

interactions. For example, the solubility of a penetrant in rubbery materials is *independent* of pressure in the absence of swelling phenomena and can be likened to a Henry's law coefficient for liquids.[11] For glassy materials, the dual-mode model has been used to describe the pressure *dependency* of the solubility coefficient.[26] This model predicts decreasing solubility coefficients with increasing pressure.

The permselectivity of penetrant A over penetrant B is the ratio of the permeability of A to the permeability of B. The permselectivity can therefore be factored into

diffusivity and solubility selectivities as shown in eq 3.

$$\frac{P_A}{P_B} = \frac{D_A}{D_B}\frac{S_A}{S_B} \quad (3)$$

Gas Permeability Studies: Fractional Free Volume. Further information regarding the relationship of structure to gas transport can be obtained by consideration of free volume effects. First, this investigation allowed comparisons to be made of the effect on permeation and selectivity of low levels of cross-linking for the organosilyl-bearing polymers. Second, the polymer density allows the specific free volume and fractional free volume to be estimated using the method of Lee,[27] which invokes the group contribution correlation of Van Krevelen[28] for the calculation of the van der Waals volumes. Chern et al.[29] and Hellums et al.[30] have shown that the ratio of specific free volume to polymer specific volume (the *fractional* free volume) gives a good representation of the degree of openness of the polymer matrix. This index takes into account the space-filling tendency of bulky side groups. The molecular weight of a single repeat unit is calculated, and the volume occupied by the atoms is estimated by summation of the various atoms present for each type of bonding and configuration. The specific *free* volume of 1 mol of repeat unit is defined as the difference between the specific volume of 1 mol of repeat unit and the summed specific *occupied* volume of 1 mol of repeat unit. The fractional free volume is then calculated as the ratio of the specific free volume to the specific volume.

Gas Permeability Studies: Permeation and Selectivity Relationships. In the present study, gas permeability values were measured and selectivity ratios determined for the series of poly(organophosphazenes) (see Tables II and III). Permeability measurements were made for helium, oxygen, nitrogen, methane, and carbon dioxide at 2-, 5-, and 10-atm pressure. However, due to the rapid development of a steady-state flux, time lags were not recorded. The brevity of the times required to attain steady-state flux with film thicknesses of 1–6 mils indicates *very high diffusion coefficients* ($\geq 10^{-8}$ cm^2/s) for these polymers. The permeabilities were scattered over a broad range of values, which is typical for rubbery and glassy polymers. By comparison, the selectivities were relatively low, even for the glassy materials.

Helium was the most permeable of the gases studied, as would be expected based on atomic diameter considerations. A significant decrease of 15.5% of the permeability for polymer **6** over the pressure range of 2–10 atm was measured. This observation is similar to the decrease of 11.7% from 100 psia to 200 psia detected for silicone rubber by Jordan et al.[31] The low modulus of these materials and the hydrostatic pressure of the upstream gas resulted in membrane compaction or free volume reduction. The critical temperature of helium is the lowest of the penetrants studied, and its extremely low solubility is consistent with the low condensability associated with such low critical temperature gases. This free volume compaction lowers the helium diffusivity in these polymers and thus decreases their permeabilities. The helium/methane selectivities varied from 2 to 27, which is low by comparison to rigid glasses. This suggests a low mobility selectivity in these high fractional free volume materials.

The permeabilities of *nitrogen* were typically independent of pressure, with three exceptions: polymer **8** showed a decrease of 8% over the range of 2–10 atm, polymer **10** showed a decrease of 20%, and polymer **14** showed a decrease of 5% over the same range. Thus, neither dual-mode behavior, which would be typical for glassy materials, nor significant free volume compaction effects as seen with helium was found. Presumably nitrogen, with a critical temperature of 126.2 K, is soluble enough to counter the tendency of the material to be compressed by the upstream feed pressure. The permeabilities ranged from 0.2 barrer for polymer **7** to over 50 barrers for polymer **5**.

The *oxygen* permeabilities varied little with pressure and ranged from 0.8 barrer for polymer **7** to 118 barrers for polymer **5**. The oxygen/nitrogen selectivity was greatest for polymers **7** and **10**, both of which contain phenyl substituents. Interestingly, replacement of a para-hydrogen atom in polymer **6** by a $SiMe_3$ group, to give polymer **8**, caused a large increase in oxygen permeability, but only a small change in the oxygen/nitrogen selectivity.

Methane in all cases experienced a higher permeability than nitrogen, and for polymers **4**, **6**, **8**, and **9** the nitrogen/methane selectivity was about 0.4. Methane, with a sieving diameter of 3.8 Å, would be expected to have lower diffusion coefficients than nitrogen, which has a sieving diameter of 3.64 Å. However, the selectivity of methane over nitrogen is typical for polymers with low diffusivity selectivities in which solubility considerations dominate. Therefore it can be concluded that methane is more soluble in these polymers than is nitrogen. This argument is consistent with the critical temperatures, 126.2 K for nitrogen and 190.9 K for methane.

The permeabilities of polymer **5** to methane increased by 8.8% over the range 2–10 atm. It is interesting to note that species **5** is also the most permeable of the rubbery polymers. The increase for this polymer is probably due to swelling induced by a high sorption level of methane. Such swelling would increase the diffusion coefficient for the methane with little or no change in the solubility coefficient.

Carbon dioxide permeability increased with pressure as a general trend, regardless of the physical characteristics of the polymer, with the exception of polymer **6**. These increases in permeability (up to 50% for polymer **14**) were accompanied by increases in the ideal carbon dioxide/methane permselectivity, but the behavior of mixed gases would probably be different. Indeed, mixed-gas permselectivities may be lower because the larger methane molecules may benefit more from the swelling of the matrix than does the more compact carbon dioxide. Even in the glassy phosphazene polymers, dual-mode behavior, in which the permeability decreases with pressure, was not detected, perhaps due to swelling at low pressures. The phenoxy substituted polymer (**6**), despite being a semicrystalline rubber (T_g = −6 °C), showed a decrease in permeability with increases in feed pressure. One possible explanation is that the degree of crystallinity in this material was sufficient to lower the sorption level of CO_2 to such a point that swelling did not occur. This hypothesis is reinforced by the relatively low CO_2 permeability found for polymer **6**.

Cross-Linking of the Poly(organosilylphosphazenes). Polymers **8**, **9**, and **10** were synthesized to probe the effects on gas transport of systematic replacement of the methyl groups by phenyl units at the silicon atoms in the para positions of the phenoxy groups. The measured glass transition temperatures did not show the anticipated increase with the increase in the degree of phenyl ring substitution of the silyl groups. The second member of the series, polymer **9**, has a T_g of 10 °C. This polymer was so mobile that it penetrated into the filter paper above the porous metal support of the permeation cell. This flow behavior caused two problems; first, the thickness of the film varied during the experiment, and second, the films failed. Fortunately, the film failures were slow and the downstream pressure transducer was never overpressur-

ized. However, permeability data could not be obtained for films of polymer **9**.

Cross-linking is a well-documented method for increasing structural integrity.[22] Films of polymers **8–10** were cross-linked by exposure to 3 Mrad of ^{60}Co γ-irradiation to yield films **8*–10***. To distinguish between the substitutional and the cross-linking effects, films of all three polymers were prepared and cross-linked in an identical fashion. The permeation behavior for the un-cross-linked films of polymers **8** and **10** was examined and was compared with the behavior of **8*–10***. The influence of cross-linking on the gas transport properties could thus be studied.

The permeabilities of polymer **8**, with trimethylsilyl groups, decreased slightly following cross-linking. The selectivities were increased slightly, which might be expected, because the cross-linked polymer would have a slightly reduced segmental mobility. The similarity between the data for the two samples is attributed to the fact that the two polymers have almost identical densities and therefore almost identical fractional free volumes as shown in Table III.

For both cross-linked **8*** and non-cross-linked **8** polymers, decreases in helium and nitrogen permeabilities with increasing pressure were observed. The explanation for this effect is similar to that used above in the discussion of the individual gases. However, the permeability to methane and carbon dioxide increased for both samples with increases in the pressure. Although the permeabilities for **8*** are slightly lower than those of the films of **8**, the pressure dependencies are very similar. The close correlations in permeability, selectivity, and pressure dependence confirm that the cross-link density in **8*** is low. This is supported by the negligible increase detected in the glass transition temperature.

As mentioned previously, gas transport studies with polymer **9** were not possible. However, the cross-linked films, **9*** were examined. The only gas which showed a pressure dependency was carbon dioxide, which displayed a permeability increase of 19%. The other gases showed no swelling effects, no free volume compaction, and of course no dual-mode behavior since this material was rubbery.

Polymer **10**, with the diphenylmethylsilyl substituents, is a glassy material. Cross-linking would be expected to create a more rigid matrix (a higher modulus), a greater resistance to swelling, and a higher number of packing defects. The permeabilities of the cross-linked films **10*** are between 39% and 67% lower than those of the films of **10**. The permselectivities were higher in all cases for the cross-linked material, with the exception of nitrogen/methane selectivities. A large difference in densities of the samples was measured as shown in Table III. Although this difference is only 2.2%, the fractional free volume difference is 8%. Typically, fractional free volumes vary from 0.08 to 0.25 between barriers and high-flux materials. Thus an 8% change would be expected to have a noticeable effect on the permeation properties.

For films of **10** the permeabilities of helium and oxygen are essentially pressure independent. The nitrogen and methane permeabilities displayed dual-mode behavior as evidenced by decreases of 20% and 11%, respectively. However, the cross-linked film (**10***) did not display such a pressure-dependent response. For carbon dioxide, films of **10** showed a permeability increase of 29% (over 2–10 atm), whereas with films of the cross-linked membranes (**10***) an increase of 34% was found. Cross-linking did decrease the permeabilities and increase the selectivities of this polymer but did not decrease the swelling effect displayed by carbon dioxide. Typically, cross-linked films would be expected to show a greater resistance to swelling; thus we assume that this sample may have been only lightly cross-linked.

The largest changes in selectivities were detected for the helium/methane gas pair. The permselectivity is presumably increased by increasing the diffusivity selectivity by cross-linking. The helium/methane solubility selectivity, although favoring methane, would be expected to increase following cross-linking. This expectation is based on the greater difficulty required to expand the matrix to accommodate the large methane molecules. Further evidence is supplied by the apparent consistency in the methane/nitrogen gas selectivities. Here diffusivity selectivity favors nitrogen but is overwhelmed by the solubility selectivity, which favors methane. After cross-linking, the solubility selectivity should decrease while diffusivity selectivity should increase.

The oxygen/nitrogen selectivity of the cross-linked sample (**10***) was about 6. This selectivity coupled with a permeability of 0.7 barrer makes the separation characteristics of this material similar to those of the glassy polymers used for the commercial separation of air. This result is surprising considering that such commercial materials are based on aromatic polymers with high glass transition temperatures.

Permselectivity of films of **10** show a pressure dependency of 43% for carbon dioxide/methane over the range from 2 to 10 atm of feed pressure. This pressure dependency can be attributed to the carbon dioxide permeability increases of 29% and methane permeability decreases of 11%. For **10*** the pressure dependency of the carbon dioxide/methane was less, at only 25%. For both samples, although the selectivity increases with pressure, a practical application would have to consider the behavior with a mixed-gas feed for which this increase in unlikely due to the typical favoring of the larger penetrant in a pair as swelling sets in.

Comparison of Silyl-Bearing Polymers. The three cross-linked samples of the silyl-containing polymers (**8*–10***) show definite trends in the permeabilities and selectivities as the phenyl ring content increases. Despite the variance in the degree of organosilyl substitution, comparisons are meaningful since the percent incorporation of each is known. Considering all of the substituent groups content and not simply the nominal designations, polymers **8–10** contain 1.97, 3.17, and 3.77 phenyl rings per repeat unit, respectively. As shown in Table III, increasing the phenyl ring content of the polymers leads to increases in density, but a concurrent increase in the fractional free volume of the polymers occurs.

Phenyl rings are flat units which can pack efficiently in phosphazene oligomer and polymer systems,[15] yet their incorporation as side groups linked to the tetrahedral silicon atoms led to packing disruptions. Despite increases in the fractional free volume, dramatic decreases in gas permeability were found. Because the phenyl rings were incorporated as terminal side units, their bulkiness could restrict the chain motions necessary for the activated process of diffusion to occur. These motions are on a smaller scale than those associated with the glass transition temperature. Although **9*** has a lower T_g and a greater fractional free volume than **8***, its permeabilities are lower. In addition, polymer **9*** displays higher selectivities than **8***, with the exception of the nitrogen/methane pair. The increases in permselectivity are presumably due to increases in diffusivity selectivity. Further increases in diffusivity selectivity would eventually lead to a nitrogen over methane permselectivity rather than a methane over nitrogen preference. This is the case with the more rigid glasses, despite the greater solubility of methane over

nitrogen. Even more inhibition to motion would be expected with the more bulky diphenylmethylsilyl groups present.

Polymer **10***, although glassy in nature, showed an increase in fractional free volume over the rubbery material **9***. The fractional free volume and phenyl ring content of polymers **9*** and **10*** are more similar than that of **8*** and **9***. Since **10*** is glassy, large differences in the transport properties would be expected as compared to either **8*** or **9***. The ratios of the permeabilities of **9*** to **10*** increase as the size of the penetrant increases. The glassy matrix of **10*** is better able to discriminate between the penetrants on the basis of size and shape. For example, the ratio of the helium permeabilities is 3.2, but the ratio of the methane permeabilities is 29. The differences in the permeability ratios of polymers **9*** and **10*** are manifested as an increase in selectivity by a factor of 10 for the helium/methane gas pair. In fact without exception, all of the selectivities for **10*** were greater than **9***.

Comparison of Transannular Ferrocenyl to Trifluoroethoxy Substituents. Polymer **14** was synthesized in a preliminary attempt to use specific interactions to enhance the permeability of certain penetrants. For example, metalloporphyrins have been incorporated as blends and as polymer chain side groups to enhance the permselectivity of oxygen over nitrogen by means of an oxygen solubility enhancement.[32-36] These attempts have met with some success but suffer from two difficulties. Stability of the carriers is a problem, with permselectivity benefits being lost after a few days or weeks.[34,35] Secondly, low-pressure saturation often occurs; thus the benefit of the carrier is usually lost at pressures greater than 1 atm.[31-35] As an additional complication, too strong an interaction can actually lower the diffusion coefficient of the preferred species.

It was considered possible that the iron of the ferrocenyl group in polymer **14** would interact only weakly with carbon dioxide or oxygen and might improve their solubilities without detrimentally affecting their diffusivities. However, the decoupling of the two factors was not accomplished and permeation measurements indicate lower permeabilities for **14** than for polymer **5** by factors of 4–12. Modest permselectivity increases were detected, but both permeability and permselectivity changes are most likely due to the fact that **14** is a glass and **5** a semicrystalline rubber.

Conclusions

A study of the relationships between polymer structure and the measured gas transport properties for a selected series of poly(organophosphazenes) was carried out. In general, the trend of high permeability accompanied by low selectivity was found. However, it was of particular interest that while the oxygen permeation values measured for poly[bis(trifluoroethoxy)phosphazene] were lower than but in the same range as those of poly(dimethylsiloxane), the permselectivity values for the phosphazene were slightly higher.

The effects of side group size, free volume, glass transition temperature, and cross-linking were examined. Despite increases in fractional free volume for the silyl-bearing polymers, decreases in permeability and increases in permselectivity were found. Overall, the phosphazene polymers used in this study provide a wide range of permeabilities and some variation in selectivity.

Experimental Section

Equipment. ^{31}P (36.2 MHz) NMR spectra were obtained with the use of a JEOL FX90Q spectrometer. ^{1}H NMR (360 MHz) and ^{31}P NMR (145.8 MHz) spectra were obtained using a Bruker WM-360 spectrometer. Chemical shifts are relative to external 85% H_3PO_4 for ^{31}P NMR and to tetramethylsilane for ^{1}H NMR. All heteronuclear NMR spectra were proton decoupled. Molecular weights were determined by use of a Hewlett-Packard HP1090 gel permeation chromatograph equipped with an HP-1037A refractive index detector and Polymer Laboratories PL gel 10-μm columns. The samples were eluted with a 0.1% by weight solution of tetra-*n*-butylammonium bromide in THF. The GPC columns were calibrated with polystyrene standards (Waters) and with fractionated samples of poly[bis(trifluoroethoxy)-phosphazene] provided by Drs. R. Singler and G. Hagnauer of the U.S. Army Materials Technology Laboratories, Watertown, MA. Thermal analyses were carried out by using a Perkin-Elmer 7 thermal analysis system equipped with a Perkin-Elmer 7500 computer. For the determination of glass transition temperatures by differential scanning calorimetry, heating rates of 10–25 °C/min under a nitrogen atmosphere were used, and sample sizes were between 10 and 30 mg.

Materials and Procedures. Standard Schlenk-line techniques, using dry argon (Matheson), were employed. THF and dioxane (Omnisolv) were dried and distilled from sodium benzophenone ketyl. *n*-Butyllithium (Aldrich), a 2.5 M solution in hexane, was used as received. The silanes (Petrarch) were freshly distilled under dry argon. Fractional sublimation at 30 °C/10 μm was utilized to purify the hexachlorocyclotriphosphazene which was provided by Ethyl Corp. The phenol (Fisher) was dried by azeotropic removal of water with benzene, the *p*-bromophenol (Kodak) by sublimation at 20 °C/10 μm. Trifluoroethanol (Halocarbon Products Corp.) was distilled under dry argon and stored over 3 Å molecular sieves. Elemental analyses were determined by Galbraith Laboratories, Knoxville, TN.

The membrane films were prepared by a solution-casting method in which a solution of the polymer in tetrahydrofuran (THF) and/or dioxane was poured onto a glass plate with the film boundaries defined by an aluminum frame. The solvent was allowed to evaporate slowly in a dust-free environment to give a homogeneous film membrane of desired size and uniform thickness. The silyl-derivatized polymers were cross-linked by exposure to 3 Mrad of ^{60}Co γ-irradiation at the Breazeale Nuclear Reactor at The Pennsylvania State University.

Permeation measurements were made using a manometric method (constant downstream volume). A Baratron type transducer from MKS was used to monitor the downstream pressure and a Heise gauge to measure the upstream pressure. A Viton O-ring sealed the upstream gas within the permeation cell. The polymer membranes were each sandwiched between two disks of aluminum foil tape to accurately define the area available for transport; areas used were either 2.84 or 9.35 cm^2. The simple average film thickness, as measured repeatedly with a micrometer, was used for the calculation of the permeability (film thicknesses varied between 1 and 6 mils). Pure gas permeability values were measured and ideal selectivities determined using standard permeation techniques as previously described.[26,37] Attempts to measure the time lag of gases upon the initial pressurization of the films were unsuccessful, indicative of rapid diffusion and consequently steady-state permeation. The gases used in the study were Linde UHP and Big 3 Industries chromatographic grades with purities of 99.97% and greater. The permeation measurements were all done at a constant temperature of 35 °C at pressures ranging from 2 to 10 atm.

Polymer densities were measured using a calcium nitrate–water density gradient column. Calibrated glass floats were used to measure the density within the column as a function of height. SYBYL 5.41a Silicon Graphics software was utilized to simulate a proton valence-filled phosphazene polymer repeat unit for subsequent calculation of the van der Waals radii (28 Å^3).

Poly[phenoxy(trifluoroethoxy)phosphazene] (4). A solution of sodium trifluoroethoxide (0.1 equiv/PCl) was added to 5.0 g of poly(dichlorophosphazene) (**3**) in THF (500 mL) and allowed to react with warming for 12 h. Subsequent addition of a solution of sodium phenoxide (2 equiv PCl) in THF to the reaction mixture followed by reflux for 12 h yielded the desired polymer **4**. The polymer was isolated by precipitation into H_2O and hexane. Purification was carried out via Soxhlet extraction in hexane for 4 days. The polymer was dried via high vacuum

to yield a white, elastomeric material (53% yield). ^{31}P NMR (THF/locked by D_2O): δ -19.7 to -17.9 (b, m). Anal. Calcd: C, 52.22; H, 3.71; N, 6.10; Cl, 1.08. Found: C, 52.41; H, 3.94; N, 5.73; Cl, 1.00. Further characterization data are found in Table I.

Poly[bis(trifluoroethoxy)phosphazene] (5). Polymer 5 was prepared by addition of excess (3.5 equiv/PCl) sodium trifluoroethoxide in 100 mL of THF to 5.0 g of poly(dichlorophosphazene) (3) in toluene (250 mL) followed by vigorous reflux for 5 h. The fully substituted polymer was isolated and purified by successive precipitations from acetone into pentane (2 times) and H_2O (2 times) followed by a final precipitation from THF into hexane. The product polymer was dried fully to give a white, fibrous material (70% yield). ^{31}P NMR ($CDCl_3$): δ -8.1 (s). Anal. Calcd: C, 19.77; H, 1.66; N, 5.76; Cl, 0.00. Found: C, 19.76; H, 1.59; N, 5.63; Cl, 0.05. See Table I for additional characterization data.

Poly[diphenoxyphosphazene] (6). Similarly, polymer 6 was prepared by the reaction of 2.5 g of poly(dichlorophosphazene) (3) in 200 mL of dioxane with excess (3 equiv/PCl) sodium phenoxide with refluxing for 48 h. The reaction solution was concentrated to 75–100 mL and the polymer isolated by precipitation into H_2O. Purification was carried out by successive precipitations from THF into H_2O (2 times) and hexane (3 times) followed by Soxhlet extraction for 2 days with MeOH. The white, fibrous polymer was dried fully under high vacuum (60% yield). ^{31}P NMR ($CDCl_3$): δ -19.1 (s). Anal. Calcd: C, 61.39; H, 4.29; N, 6.15; Cl, 0.93. Found: C, 60.28; H, 4.29; N, 6.10; Cl, 0.75. The additional characterization data are summarized in Table I.

Poly[bis(*p*-bromophenoxy)phosphazene] (7). Similarly, poly[bis(*p*-bromophenoxy)phosphazene] (7) was prepared by the addition of excess sodium *p*-bromophenoxide (3 equiv/PCl) to 15.0 g of poly(dichlorophosphazene) (3) in dioxane (200 mL) and allowed to reflux for 3 days. The polymer obtained was purified via successive precipitation in H_2O (2 times) and MeOH (2 times) followed by Soxhlet extraction with EtOH (2.5 days) and hexane (1.5 days). The white, fibrous polymer was dried under high vacuum (66% yield). ^{31}P NMR ($CDCl_3$): δ -19.7 (s). Anal. Calcd: C, 37.00; H, 2.07; N, 3.61; Cl, 0.09. Found: C, 38.59; H, 1.91; N, 3.79; Cl, <0.5. Further characterization data for this precursor polymer are summarized in Table I.

Due to the microcrystalline character of polymer 7, further reactions were carried out by initially dissolving 7 in warm THF. The reactions involving this polymer were carried out under an atmosphere of dry argon in a 1-L three-necked round-bottomed flask equipped with a mechanical stirrer. The addition funnels which contained the *n*-butyllithium and chloroorganosilane were attached to the reaction vessel prior to the cooling of the flask to -78 °C to minimize exposure of these reagents to atmospheric moisture.

Poly[(*p*-(trimethylsilyl)phenoxy)(*p*-bromophenoxy)phosphazene] (8). Polymer 7 (10.0 g, 25.7 mmol) was dissolved in dry THF (400 mL), and the solution was cooled to -78 °C (dry ice/acetone bath). To this solution *n*-butyllithium (51.4 mL of a 2.5 M solution, 0.13 mol, 2.5 equiv/site) was added. After 5 min, a solution of freshly distilled trimethylchlorosilane (32.6 mL, 0.26 mol) in THF (100 mL) was added dropwise. The reaction solution was then stirred and allowed to warm to room temperature for 12 h. The reaction mixture was then concentrated to 75–100 mL and the polymer isolated by successive precipitations into methanol (3 times) and H_2O (2 times). The polymer was then subjected to Soxhlet extraction with EtOH for 2 days. Isolation of polymer 8 gave a white, stiff, elastomeric material after vacuum drying (77% yield). ^{31}P NMR ($CDCl_3$): δ -19.3 (s). Anal. Calcd: C, 56.68; H, 6.68; N, 3.84; Br, 1.53. Found: C, 55.71; H, 6.33; N, 3.56; Br, 1.27. Additional characterization data are summarized in Table I.

Poly[(*p*-(trimethylphenylsilyl)phenoxy)(*p*-bromophenoxy)phosphazene] (9). Similarly, polymer 9 (10.0 g, 25.7 mmol) was dissolved in dry THF (500 mL), cooled, and treated as described above with *n*-butyllithium (51.4 mL, of a 2.5 M solution, 0.13 mol, 2.5 equiv/site) and dimethylphenylchlorosilane (42.5 mL, 0.26 mol). Polymer purification was achieved in a like manner as for polymer 8. The product polymer 9 was isolated as a white, stiff, elastomeric material (80% yield). ^{31}P NMR ($CDCl_3$): δ -19.5 (s). Anal. Calcd: C, 60.38; H, 5.06; N, 3.29; Br, 8.44. Found: C, 56.71; H, 5.07; N, 2.67; Br, 7.65. Further characterization data are summarized in Table I.

Poly[(*p*-(diphenylmethylsilyl)phenoxy)(*p*-bromophenoxy)phosphazene] (10). Analogously, the preparation of polymer 10 involved dissolution of polymer 7 (6.0 g, 15.4 mmol) in THF (400 mL). This was followed by treatment at -78 °C with *n*-butyllithium (30.8 mL of a 2.5 M solution, 77.1 mmol, 2.5 equiv/site) and addition of diphenylmethylchlorosilane (31.8 mL, 154.2 mmol). The polymer was isolated by precipitations into MeOH (2 times) and H_2O (2 times) followed by Soxhlet extraction in EtOH (4 days). Polymer 10 was dried to give a white, glassy material (88% yield). ^{31}P NMR ($CDCl_3$): -20.1 (s). Anal. Calcd: C, 63.39; H, 4.56; N, 3.14; Br, 8.97. Found: C, 60.95; H, 4.51; N, 2.39; Br, 8.07. Table I contains additional characterization data.

Poly[tetrakis(trifluoroethoxy)(transannular ferrocenyl)phosphazene] (14). Dilithioferrocene was prepared by reaction of ferrocene (50 g) in dry hexane (1000 mL) with *n*-butyllithium (215 mL of a 2.5 M solution, 1 equiv/site) in the presence of TMEDA (60 mL) with stirring at room temperature for 12 h. This solution was subsequently cooled to -78 °C, and excess hexafluorocyclotriphosphazene (11) (36 mL, 323.4 mmol) was added and stirred for 3 h. Additional stirring at room temperature for 48 h, gave tetrafluoro(transannular ferrocenyl)cyclotriphosphazene (12). This trimer was purified via column chromatography (hexane:CH_2Cl_2), and the isolated orange crystals were dried under vacuum to give a 22% yield of pure 12. A side product of this reaction is the formation of the pendant pentafluoro(ferrocenyl) species.

Trimer 12 (6.0 g, 15.2 mmol) was reacted with excess (2 equiv/P–F) sodium trifluoroethoxide in dioxane (300 mL) to produce the fully substituted species, 13. This [tetrakis(trifluoroethoxy)(transannular ferrocenyl)cyclotriphosphazene] was purified by column chromatography (hexane:CH_2Cl_2) and recrystallized from CH_2Cl_2:hexane under vacuum to give pure product in 83% yield (mp = 91–92 °C).

Trimer 13 was then combined with a catalytic (1 mol %) amount of hexachlorocyclotriphosphazene (2) and sealed under vacuum in a polymer tube. After 1.5 h in a 250 °C oven equipped with a platform rocker, the tube contents showed a high viscosity. The polymer was isolated under an inert atmosphere and reacted with excess sodium trifluoroethoxide (3 mmol in dioxane) at reflux for 12 h to replace any residual P–Cl bonds. The fully substituted polymer (14) was purified by successive precipitations from THF into H_2O (3 times) and hexane (2 times). The polymer (14) was dried thoroughly to yield a glassy, golden-brown material (27% yield). ^{31}P NMR (dioxane/locked by D_2O): δ 13.0, 7.4, -8.7, -13.5 (b, m). Anal. Calcd: C, 30.23; H, 2.26; N, 5.88. Found: C, 29.97; H, 2.46; N, 5.75. Further characterization data are found in Table I.

Acknowledgment. The synthesis and γ-irradiation work carried out at The Pennsylvania State University was supported by the U.S. Army Research Office and the Air Force Office of Scientific Research. The gas permeation studies carried out at The University of Texas at Austin were supported through grants provided by the Separation Research Program. The authors wish to thank R. Zauhar and C. T. Morrissey for their assistance with the molecular modeling calculations.

References and Notes

(1) Michaels, A. S. *CHEMTECH* **1989**, *19* (3), 162.
(2) Haggin, J. *Chem. Eng. News* **1990**, *68* (40), 22.
(3) Stern, S. A.; Shah, V. M.; Hardy, B. J. *J. Polym. Sci., Part B: Polym. Phys.* **1987**, *25*, 1263.
(4) Allcock, H. R. *Phosphorus–Nitrogen Compounds*; Academic Press: New York, 1972; and references cited therein.
(5) For examples of phosphazene permeation studies, see: (a) Kajiwara, M. *Sep. Sci. Technol.* **1991**, *26* (6), 841. (b) McCaffrey, R. R.; Cummings, D. G. *Sep. Sci. Technol.* **1988**, *23* (12&13), 1627. (c) Hirose, T.; Mizoguchi, K. *J. Appl. Polym. Sci.* **1991**, *43*, 891. (d) Hirose, T.; Kamiya, Y.; Mizoguchi, K. *J. Appl. Polym. Sci.* **1989**, *38*, 809. (e) Mizoguchi, K.; Kamiya, Y.; Hirose, T. *J. Polym. Sci., Part B: Polym. Phys.* **1991**, *29*, 695. (f) Kajiwara, M. *J. Mater. Sci. Lett.* **1988**, *7*, 102.
(6) Allcock, H. R.; Ewing, A. G.; Saraceno, R. A.; Riding, G. H. *J. Am. Chem. Soc.* **1988**, *110*, 7254.
(7) Martin, C. R.; Liang, W. *Chem. Mater.* **1991**, *3*, 390.

(8) Lonsdale, H. K. *J. Membr. Sci.* **1982**, *10*, 81.
(9) Graham, T. *Philos. Mag., Ser. 4* **1866**, *32*, 401.
(10) Gordon, G. A.; Ravve, A. *Polym. Eng. Sci.* **1980**, *20*, 70.
(11) Stannet, V. *J. Membr. Sci.* **1978**, *3*, 97.
(12) Higashimura, T.; Masuda, T.; Okada, M. *Polym. Bull.* **1983**, *10*, 114.
(13) Masuda, T.; Higashimura, T.; Tsuchihara, K. *J. Am. Chem. Soc.* **1991**, *113*, 8548.
(14) Allcock, H. R. *Chem. Eng. News* **1985**, *63*, 22.
(15) Allcock, H. R.; Ngo, D. C.; Parvez, M.; Visscher, K. *Inorg. Chem.*, in press. Ngo, D. C. Thesis, The Pennsylvania State University, 1991, Chapter 3.
(16) Takada, K.; Matsuya, H.; Masuda, T.; Higashimura, T. *J. Appl. Polym. Sci.* **1985**, *30*, 1605.
(17) Giglio, E.; Pompa, F.; Ripamonti, A. *J. Polym. Sci.* **1962**, *59*, 293.
(18) Allcock, H. R.; Fuller, T. J.; Evans, T. L. *Macromolecules* **1980**, *13*, 1325.
(19) Allcock, H. R.; Evans, T. L.; Fuller, T. J. *Inorg. Chem.* **1980**, *19*, 1026.
(20) Allcock, H. R.; Coggio, W. D.; Archibald, R. S.; Brennan, D. J. *Macromolecules* **1989**, *22*, 3571.
(21) Allcock, H. R.; Dodge, J. D.; Manners, I.; Riding, G. H. *J. Am. Chem. Soc.* **1991**, *113*, 9596.
(22) Allcock, H. R.; Kwon, S.; Riding, G. H.; Fitzpatrick, R. J.; Bennett, J. L. *Biomaterials* **1988**, *9*, 509.
(23) Babic, D.; Souverain, D. M.; Stannett, V. T.; Squire, D. R.; Hagnauer, G. L.; Singler, R. E. *Int. J. Rad. Appl. Instrum., C* **1986**, *28*, 169.
(24) Chern, R. T.; Koros, W. J.; Hopfenberg, H. B.; Stannett, V. T. In *Material Science of Synthetic Membranes*; ACS Symposium Series 269; Lloyd, D. R., Ed.; American Chemical Society: Washington, DC, 1985; Chapter 2.
(25) Koros, W. J.; Fleming, G. K.; Jordan, S. M.; Kim, T. H.; Hoehn, H. H. *Prog. Polym. Sci.* **1988**, *13*, 339.
(26) Koros, W. J.; Chan, A. H.; Paul, D. R. *J. Membr. Sci.* **1977**, *2*, 165.
(27) Lee, W. M. *Polym. Eng. Sci.* **1980**, *20*, 65.
(28) Van Krevelen, D. W.; Hoftyzer, P. J. In *Properties of Polymers*, 2nd ed.; Elsevier: New York, 1976; Chapter 4.
(29) Sheu, F. R.; Chern, R. T.; Stannett, V. T.; Hopfenberg, H. B. *J. Polym. Sci., Polym. Phys. Ed.* **1988**, *26*, 883.
(30) Hellums, M. W.; Koros, W. J.; Husk, G. R.; Paul, D. R. *J. Membr. Sci.* **1989**, *46*, 93.
(31) Jordan, S. M.; Koros, W. J. *J. Polym. Sci., Polym. Phys. Ed.* **1990**, *28*, 795.
(32) Nishide, H.; Ohyanagi, M.; Okada, O.; Tsuchida, E. *Macromolecules* **1986**, *19*, 495.
(33) Nishide, H.; Ohyanagi, M.; Okada, O.; Tsuchida, E. *Macromolecules* **1987**, *20*, 417.
(34) Delaney, M. S.; Reddy, D.; Wessling, R. A. *J. Membr. Sci.* **1990**, *49*, 15.
(35) Nishide, H.; Kawakami, H.; Suzuki, T.; Azechi, Y.; Tsuchida, E. *Macromolecules* **1990**, *23*, 3716.
(36) Nishide, H.; Kawakami, H.; Suzuki, T.; Azechi, Y.; Soejima, Y.; Tsuchida, E. *Macromolecules* **1991**, *24*, 6306.
(37) Chern, R. T.; Koros, W. J.; Sanders, E. S.; Chen, S. H.; Hopfenberg, H. B. *Industrial Gas Separations*; ACS Symposium Series 223; American Chemical Society: Washington, DC, 1983.